Tampere University

Vilma Heikkilä

A QUANTITIVE ANALYSIS OF SUSCEPTIBLE-INFECTED-REMOVED MODELS OF THE CORONAVIRUS

Bachelor's thesis
Faculty of medicine and health technology
Examiner: Michiel Postema
April 2021

ABSTRACT

Vilma Heikkilä: A quantitive analysis of Susceptible-Infected-Removed models of the coronavirus
Bachelor's thesis
Tampere University
Biotechnology and biomedical engineering
April 2021

Modelling the susceptibility, infection, and recovery of populations with regards to the COVID-19 pandemic is highly relevant for the implementation of countermeasures by governing bodies. Between January 1st 2020 and March 1st 2021, 13,076 COVID-19 modelling related publications were recorded in the PubMed® (National Center for Biotechnology Information of the National Library of Medicine) database. This study was conducted to assess the tools for modelling the spread of the virus. To achieve a view of the current scope of mathematical models, a selection of Susceptible-Infected-Recovered models with a focus on parameter choices was collected and quantitatively analyzed.

The models varied from simple to highly complex, with the number of used parameters ranging from one to 18. Many models included additional compartments to account for the shortcomings of a classical SIR model, but the majority also did not consider essential characteristics of the virus, such as a temporary immunity or mutated virus variants.

Keywords: COVID-19, SIR model, pandemic, mathematical modelling, virus

TIIVISTELMÄ

Vilma Heikkilä: Koronaviruksen Susceptible-Infected-Recovered-mallien kvantitatiivinen analyysi
Kandidaatintutkielma
Tampereen yliopisto
Bioteknologian ja biolääketieteen tekniikka
Huhtikuu 2021

Väestön alttiuden, sairastuvuuden sekä parantumisen mallintaminen on olennainen apuväline koronavirusta ehkäisevien toimenpiteiden toteuttamiseksi. Vuoden 2020 tammikuun ja 2021 maaliskuun välisenä aikana PubMed® -tietokantaan (National Center for Biotechnology Information of the National Library of Medicine) kirjattiin 13 076 koronaviruksen mallintamiseen liittyvää julkaisua. Tämän tutkielman tarkoituksena oli tutkia koronavirusepidemian mallintamiseen hyödynnettyjä työkaluja ja saada yleiskatsaus matemaattisen mallinnuksen tämänhetkisestä tilasta. Tutkielmaa varten koottiin laaja valikoima Susceptible-Infected-Recovered-malleja, eritoten keskittyen käytettyihin parametreihin, ja analysoitiin niitä kvantitatiivisesti.

Yksinkertaisimmissa malleissa parametreja tarvittiin yksi, kun kompleksisimman mallin parametrien lukumäärä oli 18. Monissa malleissa käytettiin ylimääräisiä väestölokeroita perinteisen SIR-mallin puutteiden paikkaamiseksi. Suurin osa malleista ei kuitenkaan huomioinut viruksen olennaisia ominaisuuksia, kuten väliaikaista immuniteettia tai uusia virusmuunnoksia.

Avainsanat: COVID-19, SIR-malli, pandemia, matemaattinen mallinnus, virus

PREFACE

This thesis was conducted in Tampere University between January and April of 2021. I would like to thank Michiel Postema for his valuable guidance throughout this work and for providing the thesis topic.

In Tampere, 27th April 2021

Vilma Heikkilä

CONTENTS

LIST OF SYMBOLS AND ABBREVIATIONS

COVID-19	Coronavirus disease 2019
SEIR	Susceptible-Exposed-Infected-Recovered
SIIR	Susceptible-Infected-Infected-Recovered
SIR	Susceptible-Infected-Recovered
SIRD	Susceptible-Infected-Recovered-Dead

1. INTRODUCTION

The coronavirus (COVID-19) pandemic conquered the world in 2020 and is still ongoing, with 110,749,023 confirmed cases reported on February 21 2021 [1]. Due to the highly contagious nature and the fast spread of COVID-19 worldwide, a need for tools to forecast the spread of the virus has emerged. Being able to evaluate the number of infections could aid governments to determine necessary precautions to slow down the pandemic and assess the needed capacity of healthcare facilities. To portray the behaviour of an epidemic with mathematical models, a few key characteristics must be considered, such as the transmission rate and the recovery rate. While any number of parameters can be added, the challenge in designing a mathematical model is estimating the actual parameter values. In the case of COVID-19, this often includes fitting the model to actual data to approximate parameter values. As the models typically focus on a specific region and use specific data sets, the parameters between models can vary greatly and lead to differences between simulation outcomes.

This study considered a set of similar mathematical models portraying the COVID-19 outbreak and compared their choice of parameters. This way, the current state of COVID-19 modelling could be evaluated. Numerous studies are being published on the subject each month, but they have not been thoroughly reviewed. The chosen mathematical models in this study focused on the Susceptible-Infected-Recovered (SIR) model and its modified derivatives.

This study is divided into six sections. In the Theory section, the fundamentals of the mathematical models are explained in more detail. The materials and methods of this study are explained in the Methodology section. The Results section introduces the chosen models and their key characteristics, and the results are discussed in the following section. Finally, a discussion about the state of mathematical models, along with a look into the future, is included in the Conclusions.

2. THEORY

2.1 Fundamentals of the SIR model

The Suscepible-Infected-Recovered model is based on earlier epidemics research [2, 3, 4, 5, 6] that propose the division of the population into compartments. The model simplifies the dynamics of the disease to its core three groups: those at risk for infection, those infectious and infected with the disease, and those no longer infected due to recovery or death. These compartments are named Susceptible, Infected, and Recovered, or alternatively, Removed. The model describes the flow of population from one compartment into another, particularly the rate of individuals getting infected and recovering from the virus. In many adaptations of the SIR model additional compartments, such as exposed and deceased, are used.

The basic model is built on a set of three ordinary differential equations describing the transfer of population from one group to the next. Each compartment is modeled as a stock of population at time *t*. A stock is a supply of people, with inflows and outflows dictating the amount of supply. The two flow rates in this model are the infection rate and the recovery rate. The infection rate is the rate of susceptible people becoming infected. In other words, it is the outflow rate from the Susceptible stock into the Infected stock. It is typically marked as [7]

$$\frac{\mathrm{d}S}{\mathrm{d}t} = -\beta IS \tag{2.1}$$

where *S* and *I* denote the Susceptible and the Infected, respectively. The transmission coefficient of a disease is typically denoted as β, and it marks the probability of transmitting the disease. From this equation it can be seen that the infection rate depends on the number of infected, the number of susceptible people that can be infected, and the transmission coefficient. β typically needs to be estimated by fitting the model to actual epidemic data.

The change in the Infected stock is described by the infection rate inflow from the Susceptible stock, and the recovery rate outflow into the Recovered stock. The rate of change is

described by the equation [7]

$$\frac{\mathrm{d}I}{\mathrm{d}t} = \beta IS - \gamma I \tag{2.2}$$

where γ denotes a recovery coefficient, which describes the rate of recovery. γ is typically the inverse of the mean duration of the illness [7].

Finally, the change in the Recovered stock is described by the inflow from the Infected stock. The recovery rate is [7]

$$\frac{\mathrm{d}R}{\mathrm{d}t} = \gamma I. \tag{2.3}$$

Sometimes $\frac{\mathrm{d}S}{\mathrm{d}t}$ and $\frac{\mathrm{d}I}{\mathrm{d}t}$ are also expressed as

$$\frac{\mathrm{d}S}{\mathrm{d}t} = -\beta \frac{I}{N} S, \tag{2.4}$$

and

$$\frac{\mathrm{d}I}{\mathrm{d}t} = \beta \frac{I}{N} S - \gamma I \tag{2.5}$$

where N is the total population and the sum of the three compartments. In these equations the infected compartment is considered as a proportion of the total population.

Figure 2.1 represents the model in a typical stock and flows diagram (a), and in terms of the model outputs (b). The output diagram shows the number of people in each compartment on a given day.

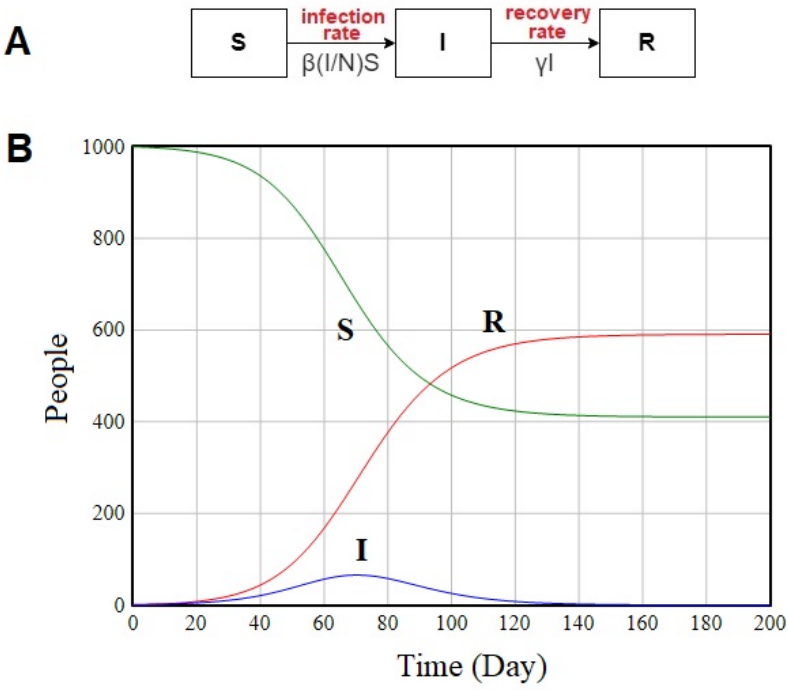

Figure 2.1. *A stock and flows diagram (A) and output diagram (B) for a typical SIR model.*

A few assumptions are made with this model. Namely, that the susceptible population is homogenous, the transmission rate is constant throughout the epidemic, and once recovered, an individual is immune to the disease and removed from the model. This could prove problematic with COVID-19 for a few reasons. Firstly, a population is rarely homogenous throughout a region. Secondly, government intervention can affect the transmission rate of the virus. Lastly, there is conflicting and limited data on whether infection actually grants immunity [8], and permanent immunity should not be assumed. Thus, some adaptations of the model include a time-varying transmission rate or a gradual loss of immunity for the recovered population.

2.2 Modified SIR models

Many types of compartmental models have been derived from the classical SIR model. The most common ones include the Susceptible-Infected-Recovered-Dead (SIRD), the Susceptible-Exposed-Infected-Recovered (SEIR), and the Susceptible-Infected-Infected-Recovered (SIIR) model. A SIRD model includes an extra compartment for fatalities resulting from the virus, with the transfer rate often being described by an equation such as

$$\frac{\mathrm{d}D}{\mathrm{d}t} = dI, \tag{2.6}$$

where d would denote the fatality rate. Similarly for SIIR models, the infected compartment in SIIR models is divided into two or more groups, such as asymptomatic and symptomatic. Any additional compartments can be used, such as the quarantined or hospitalized populations. Typically all compartments would have their own transfer rates, similarly to the fatality rate in SIRD models. In more complex models, these rates are not necessarily a single parameter, and could have multiple coefficients taken into account, or even include time-varying variables.

2.3 Vensim simulations

Vensim® is a simulation software developed by Ventama Systems, capable of solving systems of differential equations. As showcased in the previous sections, SIR models consist of differential equations, so Vensim is a fitting tool for simulations with this type of model.

Keeping in mind the structure of the basic SIR model, the modelling process in Vensim can be demonstrated. A population, or a stock, is portrayed by a level variable. The value of a level variable changes dynamically, and is determined by its initial value and an equation defining the inflows and outflows of population. The model parameters in a simple SIR model like the one presented here can be implemented as a normal variable with a constant value. Next, the transfer of population between these stocks is implemented as a rate, indicated by an arrow determining the flow direction and defined by an equation. Figure 2.2 shows a Vensim model representing the system defined by equations (2.1–2.3), where the infection rate is portrayed by (2.1) and the recovery rate by (2.3). It can be seen that in Vensim each variable affecting an equation must be connected to the equation by an arrow. After the model structure has been established, the only thing left is inserting the appropriate stock initial values and parameter values.

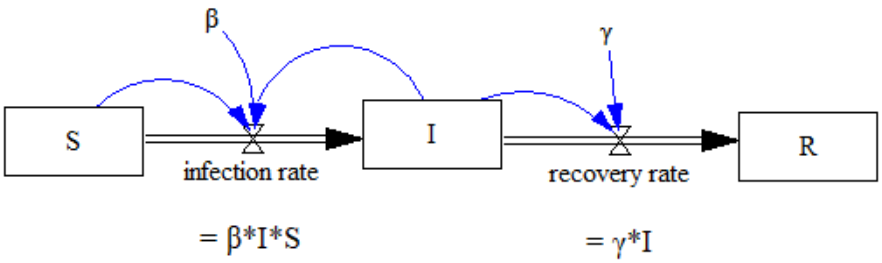

Figure 2.2. *An example model created in Vensim.*

3. METHODOLOGY

This study featured both a literature review segment and a practical segment. A selection of suitable papers needed to be collected and reviewed to assess their models. Once this was done, recreations of models from these papers could be attempted to evaluate the simulation process.

3.1 Literature review

The selected papers were found in the PubMed online database, using queries such as "(COVID-19) AND (SIR model)". The timeline was limited to the last 14 months, spanning from January 2020 to March 2021. The search was especially focused on extended models, such as models with additional compartments and additional or time-variant parameters. Papers with unclear model characteristics, or those otherwise inapplicable for the purposes of this study, were excluded.

The models were organized in a table in an order of increasing number of parameters.

3.2 Simulations

The simulation of seven select models was showcased. The models were recreated as presented in the papers using the personal learning edition (PLE) of Vensim. Equations were inferred from the papers to assess whether the presented results could be achieved as such. Recreating the models also offered insight of their complexity, such as the number of variables needed.

4. RESULTS

This section focuses on the analysis of the models, specifically the type of model and parameter choices. The selected models and their parameters are organized in Table A.1 in the Appendix by number of parameters used. Additionally, a list of excluded studies is included.

4.1 Models in detail

Here the details of each model are briefly discussed. The simplest models are showcased first before getting familiar with increasingly complex ones.

4.1.1 One-parameter models

Katul et al. [9] used a SIR model which they normalized by the recovery rate γ and the initial condition S_0. The parameter used in this model was the basic reproduction number R_0 that they used for simulating the epidemic in 57 countries, but which globally converged to 4.5.

Sadurní and Luna-Acosta [10] reduced a simple SIR model to a one-variable system and ran simulations with varying values of the control parameter κ.

4.1.2 Two-parameter models

Ahmetolan et al. [11] used a classical SIR model, but as parameters they used the basic reproduction ratio R_0 which was the ratio of the infection rate and the removal rate, and the mean infectious period T, which was the reciprocal of the removal rate. The parameter ranges were $1.5 < R_0 < 10$ and $2 < T < 30$. They modelled the epidemic in China, South Korea, France, Germany, Italy, Spain, Iran, Turkey, the United Kingdom, and the United States.

Al-Anzi et al. [12] simulated the epidemic in the United States, Brazil, India, China, Switzerland, Ireland, and Kuwait using a classical SIR model. They used a MATLAB SIR modeling tool that estimated the model parameters based on daily new infections.

Barlow and Weinstein [13] applied a typical SIR model to the case of Japan with the parameters transmission rate r as 2.9236×10^{-5} and the recovery rate α as 0.0164.

Dos Santos et al. [14] included an infection rate $\beta(t)$ which ran within $[0.05, 0.6]$, and a recovery rate $\gamma(t)$ which ran in range $[0.07, 0.13]$. The model was applied to Germany, Italy, France, and the United Kingdom.

Jung et al. [15] combined the use of neural networks and a SIR model with time variant parameters, the infection rate β and the recovery rate γ, to portray the epidemic in South Korea. Their model assumed the total population number to remain unchanged for the duration of the simulation. For the whole country, the parameter values were estimated as 0.1656 for β, and 0.0253 for γ. They repeated the simulation for Seoul, Busan, Daegu, and Gyeonggi.

Lounis and Bagal [16] used a simple SIR model to simulate the epidemic in Algeria. They estimated the transmission rate β as 0.0561215 and the removal rate γ as 0.0455331. They assumed that the total population number would remain unchanged.

Malavika et al. [17] used a basic SIR model to model the epidemic in India. Their transmission parameter β was 0.36 and the recovery rate γ was 0.14. The model focused on the very early dynamic of the epidemic in February—May.

Miranda et al. [18] combined a regular SIR model with a network diffusion model and applied it to Brazil. Their parameters included transmission rates β_i, β_s, and β_c for municipality, state, and the whole country, and the recovery rate γ.

Nguemdjo et al. [19] simulated the epidemic in Cameroon using a simple SIR model. Their effective contact rate β was 0.36 and the removal rate γ was 0.393. They considered the whole population, except for the initial infected individual, susceptible.

Srivastava et al. [20] modelled scenarios with different effects of lockdown in India using an SIR model. The best fit values of the parameters contact rate r and recovery rate a were stated as 0.0096 and 0.1006, respectively. They also discussed the inclusion of birth and death rates and the migration of population, but any values for parameterizing these effects were not estimated.

Szapudi [21] used a SIR model which considered heterogeneity by taking into account the number of links an individual has to other persons. Their model included the parameters infection probability β as 0.07 and the recovery rate γ as 0.1.

Turk et al. [22] simulated the epidemic in North Carolina (NC) and the greater Charlotte Region (CRI) in the United States with an SIR model. They estimated the infection rate β and the removal rate γ twice for both regions: β values were 0.6415 and 0.6165 for NC, 0.7020 and 0.6381 for CRI, and the γ values were 0.3585 for NC, and 0.2980 and 0.3619 for CRI.

4.1.3 Three-parameter models

Abuhasel et al. [23] created a classical SIR model representing the Kingdom of Saudi Arabia, with the contact rate β being 0.133 and, recovery rate γ being $\frac{1}{14}$, and the population N being $34,806,116$. They assumed that the whole population would be susceptible at the start. To account for deaths, the SIR model was combined with a SIRD model, but no parameters or results were shown for this modified model.

Ambrosio and Aziz-Alaoui [24] modelled the epidemic in the New York state of the United States, using a SIRD model with parameters that were adjusted over time. The recovery rate r was set at a constant 0.64, while the infection rate k varied at 1.047—0.67 and the death rate d at 0.0016—0.00232. They also integrated people commuting from New Jersey to New York by coupling two SIR systems. This was implemented by introducing periodic functions for population densities.

Amiri Mehra et al. [25] first used a simple SIRD model to simulate the epidemic in South Korea and in the United States. For South Korea, they estimated the transmission rate β as approximately 1, the recovery rate g as 0.223, and the removal rate μ_d as 0.0261. Their other model with more parameters will be introduced later on.

Enrique Amaro et al. [26] used an SI model with an extension for deaths, which did not consider recoveries. The model employed the parameters a for the theoretical number of deaths, b for the characteristic evolution time, and c for an inverse dead factor.

Fanelli and Piazza [27] used a very simple SIRD model to simulate the situation in Italy and China. The parameters were as such: for Italy, the infection rate r was 7.9×10^{-6}, the recovery rate a was $2.13 \times 10-2$, the death rate d was 1.63×10^{-2}, and for China they were $3.33 \times 10^{-6}, 1.8 \times 10^{-2}$ and 3×10^{-3}.

Fort et al. [28] developed a model for estimating hospital capacity, and included variables for susceptible, infected, recovered, symptomatic, incubating, hospitalized patients, patients requiring intensive care, patients requiring mechanical ventilation, patients requiring inpatient admission, calculated totals for the Greater New Orleans Metropolitan Area, and patients discharged. Parameters included the basic recovery rate R_0, contacts per unit time β, and the inverse of the mean recovery time, γ.

Guirao [29] created a simple SEIR model and applied it to Spain, Italy, and Germany. The presented model used the parameters reproductive number r_0, infection period τ_i, and latent period τ_l. Two values for parameters were inferred, so τ_i values were 1.63 and 2.56, and τ_l values were 3.0 and 2.0.

Harb and Harb [30] created a theoretical SIRD model with the parameters contact factor

b, transmit factor a, and a health medication quality factor m which affected the probability of death. No explicit values were given for the model parameters.

Ianni and Rossi [31] modelled the epidemic in Italy and Germany for the first half of 2020 using a time variant SIRD model. The used parameters were as follows: for Italy, the initial transmission rate β_0 was $\frac{1}{1.8}$, the recovery rate γ_R was $\frac{1}{41}$, and the mortality rate γ_D was $\frac{1}{145}$, and for Germany they were $\frac{1}{2.2}$ for β_0, but the other parameters were not given values. Their SIIR model will be presented later on.

Law et al. [32] simulated the epidemic dynamics in Malaysia with time variant parameters. zB_t was the partial transmission coefficient at time t, where B_t was defined by the proportion of depletion p and scaled by a fraction z, and the removal rate was δ. The parameter values were fitted three times, where the values of z were $0.4374, 0.3914$, and 0.4047, the values of p were $0.0784, 0.0450$, and 0.0466, and the values of δ were $0.025, 0.042$, and 0.050.

Mohamed et al. [33] included an M compartment for immune people or those who will be unaffected by the virus and applied their model to the three cities, Riyadh, Hufof, and Jeddah, in the Kingdom of Saudi Arabia. Their model included the parameters infection rate β, recovery rate γ, and the number of unaffected people α.

Roda et al. [34] presented two models to portray the epidemic in Wuhan, China. First they used a simple SIR model with the transmission rate β as 9.906×10^{-8}, the diagnosis as ρ being 0.24, and the recovery rate μ as 0.1. R denoted the confirmed cases. They stated that deaths of susceptible and infected individuals were negligible, and they seemingly considered a death rate for the R population, but no parameter value for it was given. The second model, a SEIR model, will be discussed later.

Rubin et al. [35] showcased a SIIR model which introduced a mutation of the virus at day 60. The infected population was divided into the primary infected, and the infected with the mutation. Their parameters included a transmission constant β as 0.19, the recovery constant γ as 0.125, and an infectiousness multiplier 1.5, which described the heightened infectiousness of the new mutation.

Wangping et al. [36] used time-varying parameters in their SIR model by including a transmission modifier π, the value of which varied depending on intervention measures. The transmission rate β was then modified by this parameter. A removal rate γ parameter was also used. They applied their model to Italy and Hunan, China.

Zareie et al. [37] used a SIR model with time-dependent parameters transmission rate $\beta(t)$, recovery rate $Y(t)$, and death rate $\mu(t)$.

4.1.4 Four-parameter models

Alanazi et al. [38] added a level of complexity by introducing what they called a SIR-F model, which was essentially a SIRD model. Their last parameter fitting gave the following parameter values: the effective contact rate β was 0.1, the mortality rates α_1 and α_2 were 0.018 and $\frac{1}{47464}$, and the recovery rate γ was $\frac{1}{17}$.

Calafiore et al. [39] modelled the epidemic in Italy using a SIRD model with time-varying parameters. The parameters were as follows: the infection rate β varied approximately in range $[0.63, 0]$, the recovery rate γ approximately in range $[0, 0.048]$, and the death rate ν in range $[0, 0.08]$. They used a scalar parameter $q \in [0, 1]$.

As mentioned, Ianni and Rossi [31] also created a SIIR model in which they considered the asymptomatic cases of the virus, but not deaths. The model employed four parameters, which were the transmission rates β_S and β_A for the symptomatic and asymptomatic infected populations, and similarly, the recovery rates γ_S and γ_A. The initial transmission rate β_0 was $\frac{1}{5}$, β_A was $\frac{1}{7}$, γ_S was $\frac{1}{41}$, and γ_A was $\frac{1}{78}$.

Kobayashi et al. [40] combined a state space model with a simple SIR model. The unknown parameters of their model were the infection rate β, the recovery rate γ, and two parameters determining randomness in the model, κ and λ.

Kolokolnikov and Iron [41] integrated spatial distribution of population into their modified SIR model, which they showcased for the world, the United States, Canada, and Russia. For the world, they estimated the parameters total population N as 7.7×10^9, an infection parameter α as 15050, rate of interaction μ as 1.25×10^{-5}, and the recovery rate γ as 0.0232.

Maier and Brockmann [42] created a SIRQ model for Hubei, China, that considered the quarantining of infectious individuals. The best fit parameters for the basic reproduction number R_0 was 6.2, and for the infection period T_I it was 8. They simulated scenarios with varying containment rates k and k_0.

Moussaoui and Zerga [43] created a SIR model which considered intervention strategies in Algeria, that is, different levels of mask wearing m and social distancing d. They also considered the level of protection from masks, e, and the basic reproduction number R_0.

Peng et al. [44] used an SIR model for China that considered the proportion of unquarantined infected individuals α. Their transmission rate composed of the effective contacts with infected individuals per day $\lambda = 5$ and the infection probability $p = 0.040$, and their recovery rate was $\mu = \frac{1}{14}$.

Prodanov [45] normalized a SIR model to include both the transmission rate and the recovery rate in the parameter g, which was also the reciprocal of the reproductive number R_0. They also fitted the parameters i_m for the apparent peak of incidences and fatalities,

and the apparent peak times T for them. The model was applied to Bulgaria, Belgium, Netherlands, Germany, and Italy.

Rocchi et al. [46] considered the asymptomatic individuals and the immunity loss in their SIIR model. They used the parameter values 0.6 for the infection rate α and 0.1 for the removal rate β, and their immunity loss rate ρ varied from 0.003 to 0.006 and the proportion of symptomatic individuals p varied from 0.01 to 0.10.

The second model by Roda et al. [34] was a SEIR model where individuals in E were infected but not infectious. The parameters were β as 8.68×10^{-8}, ρ as 0.018, μ as 0.1, and the transfer rate from the exposed population to the infected population, ϵ, as 0.631.

4.1.5 Five-parameter models

As mentioned before, Amiri Mehra et al. [25] also proposed a Susceptible-Infected-Infected-Recovered-Quarantined (SIIRQ) model, which considered presymptomatics and quarantined individuals in the previous countries. They considered scenarios with a 0.95 quarantine rate ϕ, and the other parameter values for South Korea were approximately 1 for the transmission rate β, 0.214 for the transfer rate α between the presymptomatic and infected population, 0.222 for the recovery rate g, and the removal rate μ_d.

Brandenburg [47] constructed a SIR model with a spatial extension. The model parameters were reproduction rate λ, recovery rate μ, and a diffusion constant κ. Additionally, they considered the spatial and temporal coordinates x and t.

Brugnano et al. [48] used a multiregional SIIR model to simulate the epidemic in Italy. As parameters the model had the infection rate β_i, the removal rates γ_{i1} for undiagnosed infected individuals and γ_{i2} for diagnosed infected individuals, the probability of detecting an infection σ_i, and a delay time τ to account for the time between an onset infection and the detection of the infection. The country was divided into four regions, and i signified the region. All other parameters were free, except for $\gamma_1 = 0.043$ and $\tau = 10$.

Cooper et al. [49] modelled the epidemic with a SIRD model in Italy, India, South Korea, and Iran. To account for population moving around, it was possible to increase the number of susceptible individuals. The parameters of the model were the transmission rate a, the removal rate b, and death constants D_0 and k_0 with which the deaths were estimated from the removed population. For Italy, the parameter values were $a = 0.18, b = 0.037, D_0 = 3.6 \times 104$, $k_0 = 1.6 \times 10^{-5}$ and $f = 2.4 \times 10^5$.

Zhao and Chen [50] created a Susceptible-Unquarantined-Quarantined-Confirmed model with the parameters infection rate α, quarantine rate γ_1, and three confirmation rates γ_2, σ, and δ. α was said to be calculated as 0.2967, and the other parameters were es-

timated for Beijing, Shanghai, Guangzhou, and Shenzhen, in two stages for each. The stage 1 estimation for Beijing for γ_1, for example, was 0.3357. A confirmation rate for this was estimated the value 0.0906, but it was not specified which rate this was.

4.1.6 Models with six to seven parameters

Bastos and Cajueiro [51] modelled the early evolution of the virus in Brazil. They used what they called a SIRASD (Susceptible-Infected-Recovered-Asymptomatic-Dead) model, which here was categorized as a SIIRD model. Their model featured seven parameters: the infection rates $\beta_S = 0.4417$ for symptomatic people and $\beta_A = 0.4417$ for asymptomatic people, the removal rates $\gamma_S = 0.1508$ for symptomatics and $\gamma_A = 0.1260$ for asymptomatics, the proportion of the symptomatic $p = 0.3210$, the probability of death $\rho = 0.0347$, and the effectiveness of social distancing $\psi \in [0, 1]$.

Berestycki et al. [52] proposed a Susceptible-Infected-Recovered-Travelling model. They included diffusion of population by introducing a road: a line that people travel on. Their model parameters included diffusion coefficients d for the Infected population and D for the Travelling population, the transmission rate β, recovery rate α, and exchange coefficients μ for giving individuals to a region and ν for receiving individuals from a region. No explicit parameter values were given.

Nakamura et al. [53] reduced the basic model into a single first-order differential equation, focused on accumulated deaths in their SIRD model by introducing a sigmoid expression in the model. The model included the parameters transmission rates β, removal rate λ, mortality rate f and the sigmoid parameters τ, g_∞, and b. The model was applied to France, Denmark, Italy, Spain, the United Kingdom, Germany, and Belgium.

Karaivanov [54] also used neural networks in their SEIRD model. In their model, the probability of infection was heterogenous between individuals. Their parameters included the infectivity rate β of 0.5, the removal rate r of 0.2, the mortality rate μ of 0.00074, the recovery rate γ of 1.9926, an incubation parameter σ of $\frac{1}{5.2}$, the mass testing rate θ of $2\%, 5\%$, and the contact tracing rate ϕ of 10%.

Neves and Guerrero [55] proposed an SIIRD model with asymptomatic and symptomatic infected populations, which they applied to Lombardy, Italy, and São Paulo, Brazil. They considered the parameters transmission rate β_0, a reduction factor μ for the transmission rate, the probability of developing symptoms ξ, the removal rates γ_s and γ_a for the symptomatic and asymptomatic cases, the case fatality rate ω, and the intensity of implemented control measures ϵ.

4.1.7 Models with 9 to 11 parameters

Batistela et al. [56] considered immunity loss and the effect of social distancing in their SIIR model, which had compartments for unreported and asymptomatic infections, and confirmed infections. They applied their model to three Brazilian cities, São Paulo, Santos, and Campinas with five fits for parameters. For example, their first fit for São Paulo was as follows: birth rate λ as 3.595×10^{-5}, death rate δ as $\delta = 1.822 \times 10^{-5}$, infection rate α as 0.9377, removal rate σ as 0.1117, the recovery rates β_1 and β_3 as 0.1181 and 0.06325, the diagnosis rate β_2 as 0.2978, the effect of social distancing θ as 0.5005, and the immunity loss rate γ of 3.595×10^{-5}.

Tomochi and Kono [57] used an SIIR model to simulate the epidemic in Japan. Their model had two Infected compartments for presymptomatic individuals and symptomatic individuals, and three Removed compartments for infected but quarantined individuals, the recovered individuals, and the fatalities. They coupled two of these SIIR systems to account for a second wave. For the systems, the transmission rate β was 0.16, the transfer rates b_1, b_2 were 0.012, and 0.188, the transfer rates c_1, c_2, c_3 were $\frac{1}{17}$, $\frac{0.942}{17}$, and $\frac{1}{17} - \frac{0.942}{17}$. The immunity loss rate, or the inverse of the antibody duration, d_1, was 0, the incubation period t_1 was 5, and the onset period t_2 was 17.

Venkatasen et al. [58] used an SIRD model to portray the epidemic in India. They used the parameters transmission rate which had its measured value vary approximately in range $[0.02, 0.5]$, fraction of susceptible, a contact success rate of 0.1, infected contacts, a contact rate of 10, an illness duration of 14 days, a growth rate of 0.28, a reproduction ratio, and a fatality ratio, of which the measured value varied in range $[0.01, 0.04]$.

The SIR model by Muñoz-Fernández et al. [59] featured a non-constant transmission rate β, death rate μ', and γ. They also included a general birth rate λ and a general death rate μ. For estimating the values of the transmission and death rates, coefficients $a_\beta, a_{\mu'}, b_\beta$, and $b_{\mu'}$ were used. They applied the model to the cases of Italy, Spain, and the United States.

Carli et al. [60] proposed a multi-compartmental and multi-regional Susceptible-Infected-Removed-Quarantined-Threatened-Healed-Extinct model. Their parameters were the infection rate $\beta(k)_i$, the diagnosis rate θ_i, the healing rates $\gamma_i, \delta_i, \pi_i$ for the infected, quarantined, and threatened individuals, the hospitalization rates λ_i, μ_i for the infected and quarantined individuals, and the death rate ϵ_i for the ith region. They also had a migration coefficient $\xi_{I,j}$ from region i to j, and intra-regional and inter-regional restrictions $U_i = [0, 0.2, 0.8]$ and $R_i = [0, 1]$, respectively.

Peng et al. [61] introduced an SIIR model with time-varying transfer rates: undocumented infection rate, transmission rate and infection fatality rate, and estimated their values based on data from the United States. In their study they used the parameters

infection rate β, recovery/death rate λ, unreported infection rates ϕ and ϕ', coefficients a, b, c, d and constants m, n and k.

4.1.8 Models with 12 or more parameters

Colombo et al. [62] created a Susceptible-Infected-Hospitalized-Recovered model with age and space dependent parameters, with the parameters hospitalization or quarantining rate κ, recovery rates θ and η, mortality rates $\mu_S, \mu_I, \mu H,$ and μ_R, and a disease transmission function ρ with position variables x and ξ, and age variables a and α.

Ibarra-Vega [63] used a SIRD model to simulate theoretical scenarios, which had a long lockdown, two short lockdowns and one smart lockdown, one medium lockdown and one smart lockdown, and no lock down. The parameters they listed were contacts rate μ, the fatality rate Fr, the hospital capacity strain index HiC, the incubation time it, the disease duration Dd, the fraction requiring hospitalization Fh, infectivity β, hospital capacity HC, lockdown effectivity λ, smart lockdown effectivity k, post-lockdown effectivity q, and serious cases SC. No numerical values were given for these parameters.

Ferchiou et al. [64] constructed a 15-parameter model with compartments for susceptible, exposed, infectious, hospitalized, in intensive care units, recovered, and dead. The infected compartment was further divided into asymptomatic, paucisymptomatic, and those having mild or severe symptoms. Their parameters were the incubation period θ^{-1} as 5.2, the prodromal phase duration μ_p^{-1} as 1.5, the latency period ϵ^{-1} as 3.7, the probability of being asymptomatic Pa as 0.2, the probability of being paucisymptomatic Pps as 1 for children and 0.2 for adults, the probability of having mild symptoms Pms as 0 for children, 0.7 for adults, and 0.6 for seniors, the probability of having severe symptoms Pss as 0 for children, 0.1 for adults, and 0.2 for seniors, the serial interval s as 7.5, the infectious period μ^{-1} as 2.3, relative infectiousness r_β as 0.51, the probability of going in ICU $pICU$ as 0 for children, 0.36 for adults, and 0.2 for seniors, the raily rate of recovery for hospitalized individuals $\lambda_{H,R}$ as 0 for children, 0.072 for adults, and 0.022 for seniors, the daily rate of recovery for those in an ICU $\lambda_{ICU,R}$ as 0 for children, 0.05 for adults, and 0.036 for seniors, the daily death rate for hospitalized individuals $\lambda_{H,D}$ as 0 for children, 0.0042 for adults, and 0.014 for seniors, and finally, the daily death rate for those in an ICU $\lambda_{ICU,D}$ as 0 for children, 0.0074 for adults, and 0.029 for seniors.

Ramos et al. [65] presented the most complex model thus far with 18 parameters, the θ-Susceptible-Exposed-Infected-Hospitalized-Quarantined-Recovered model, where θ was the proportion of undetected infections. Other parameters included were population N as $60,317,000$, transition rates γ_E as $\frac{1}{5.5}$, $\gamma_I(t)$ as $\frac{1}{5}$, $\gamma_{I_u}(t)$ as $\frac{1}{9}$, $\gamma_{H_R}(t)$ as $\frac{1}{14.2729}$, $\gamma_{H_D}(t)$ as $\frac{1}{5}$, $\gamma_{I_{Du}}(t)$ as ∞, $\gamma_{Q,1}$ as $\frac{1}{36.0450}$, $\gamma_{Q,2}$ as $\frac{1}{24.88646}$, disease contact rates $\beta_{I,0}$ as 0.4992, $\beta_{I_{Du},0}, \beta_{H_R}, \beta_{H_D}$, instantaneous infection undetected fatality ratios $\omega_{u,0}, \omega_{u,1}$ and $\omega_{u,2}$ as

0.42, 0.42, and 0, and the ratio of new detected infected who will recover after hospitalization p_0 as 0.7382.

4.2 Recreated simulations

An interesting experiment to conduct using these models is trying to recreate them as was presented to assess the simulation process and examine whether achieving similar results as such is possible.

The Abuhasel [23] model was simple to recreate, with the initial conditions being $S(0) = N - I(0)$, $I(0) = 387$, and $R(0) = 0$, where N was $34,806,116$. The simulation took three parameters. The recreated results can be seen in Figure 4.1.

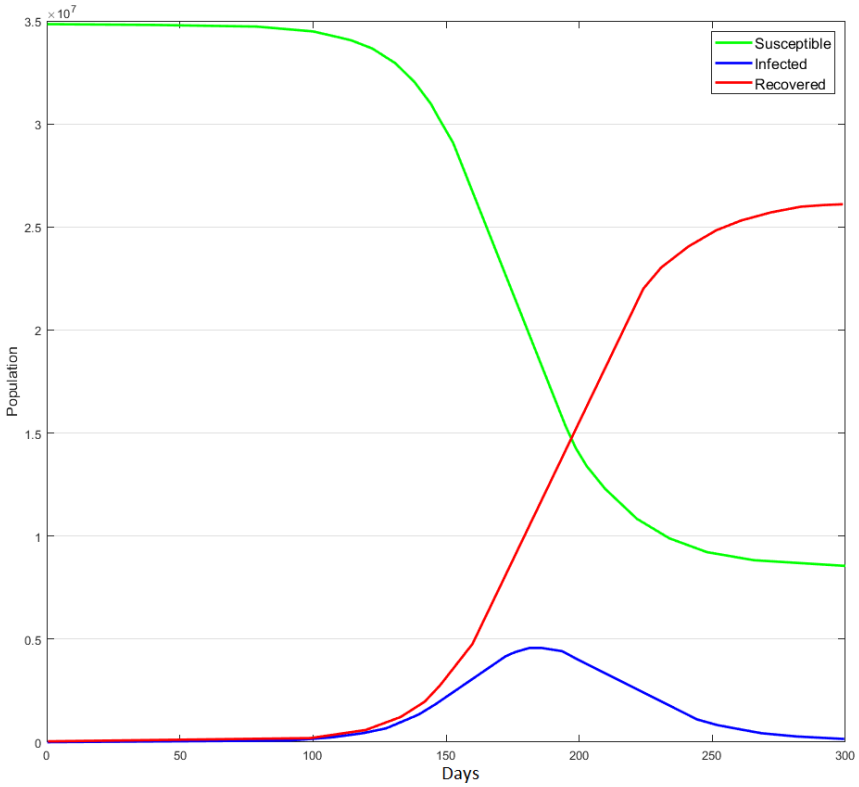

Figure 4.1. *The Abuhasel [23] model results recreated in Vensim.*

For the Nguemdjo [19] model the given initial conditions were $(S(0), I(0), R(0)) = (N - 1, 1, 0)$, where the population size was $N = 25,216,237$. The model was recreatable with the given information, and it only needed to be normalized by the total population to achive the same results. Recreating the model took three parameters in total. A Vensim recreation of the results is in Figure 4.2.

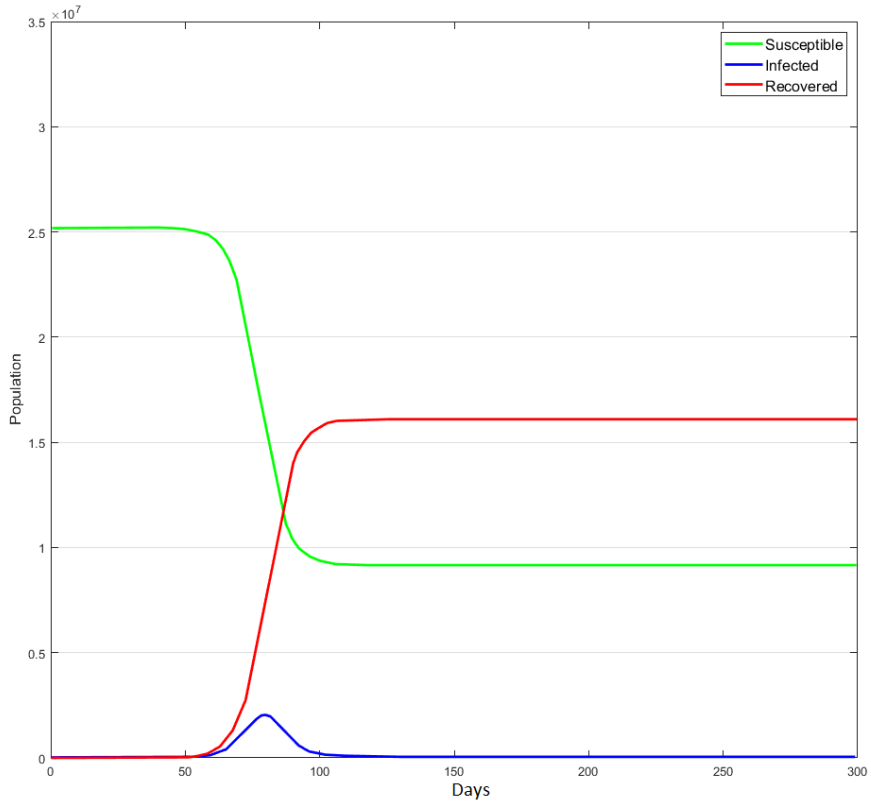

Figure 4.2. *The Nguemdjo [19] model results recreated in Vensim.*

The results of the Fanelli and Piazza [27] model were recreatable with the given parameter values and the given initial conditions $S(0) = 4.13 \times 10^4$, $I(0) = 3$, $R(0) = 0$, and $D(0) = 0$ for Italy. This model was as simple as a SIR model with additional compartments could get, with only four parameters used. This included a parameter determining the onset period of the epidemic. The recreated results for Italy can be seen in Figure 4.3.

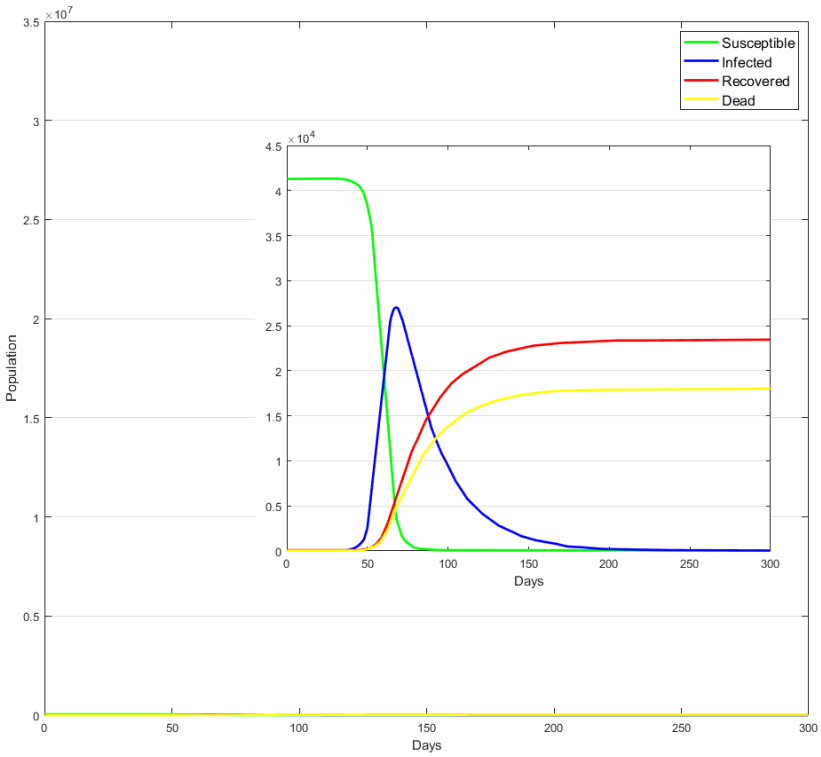

Figure 4.3. *The Fanelli and Piazza [27] model results recreated in Vensim.*

The initial conditions used in the model by Law [32] were $S(0) = 32,680,000$, $I(0) = 90$, and $R(0) = 62$. The model for each fit was easily recreatable with the given parameters, of which the final fit can be seen in Figure 4.4. There did not seem to be a value listed for the initial transmission rate $B_{t=0}$, but using a value of $B_{t=0} = 0.4114$, a value that was mentioned earlier in their paper, gave similar enough results. Six parameters were used to recreate this model.

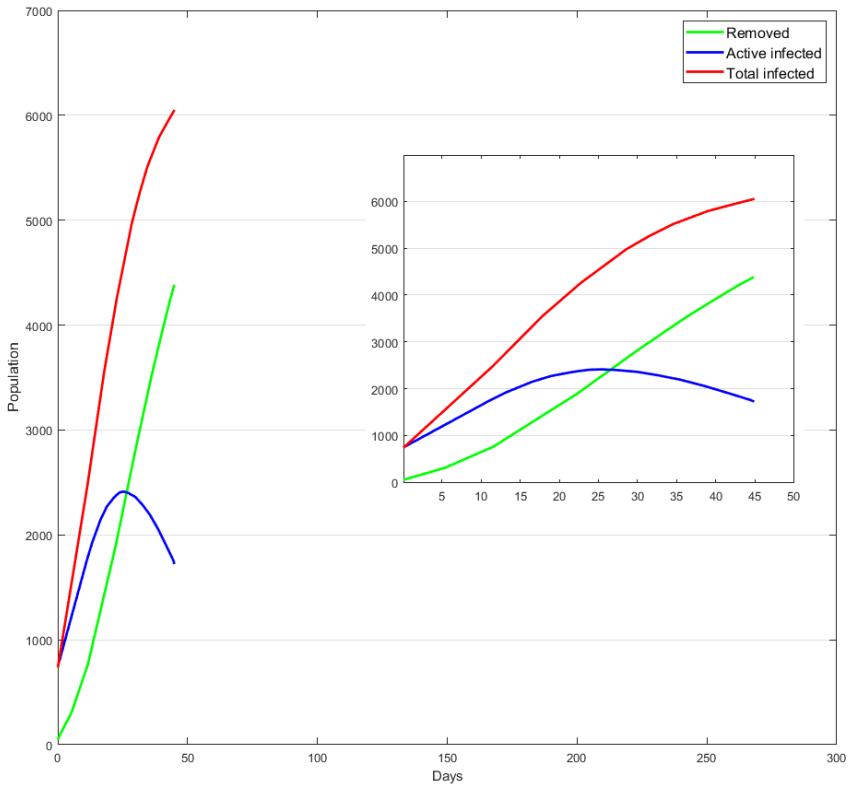

Figure 4.4. *The Law [32] model results recreated in Vensim.*

Not all models could be created solely based on information presented in the papers. In some cases all variable values were not reported or the model was not built the way they were presented and some tweaking needed to be done, or they the results could not be recreated at all.

For instance, in the Malavika [17] model no initial values for the compartments were given, so it could not be tested on Vensim as such. Using a total population number of 1.38 billion and initial values of 0.685, 1 over 1.38 billion, and 0 for Susceptible, Infected and Recovered, respectively, it was possible to achieve 57,450 active infections on around May 18 as was reported. Three parameters were used, one of which was the population number used to scale the Infected compartment. The recreated results are in Figure 4.5.

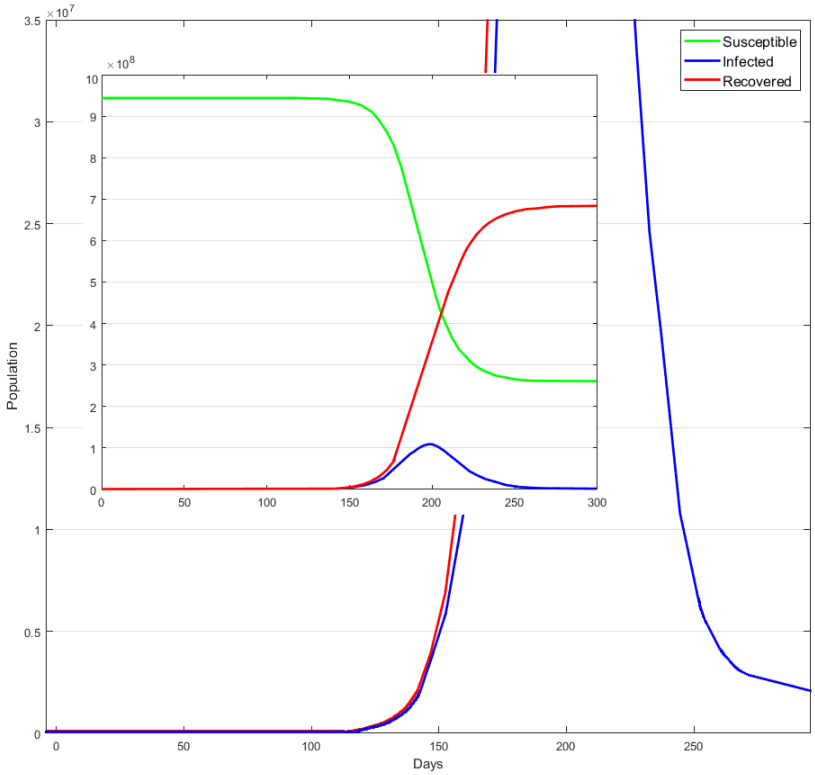

Figure 4.5. *The Malavika [17] model results recreated in Vensim.*

The given inital conditions for the Cooper [49] model were $I(0) = 1.3 \times 10^{-3}$ and $R(0) = 6.21 \times 10^{-4}$. As there was no explicit initial value given for the Susceptible compartment, nor were values given for the surges, the model could not be recreated outright. Assuming $S(0) = 1$ gave a similar result for the first wave in Italy, specifically the infected compartment. For India, continuous surges would need to be added to achieve the correct result. Five parameters were needed in this simulation. The recreation results for Italy can be seen in Figure 4.6.

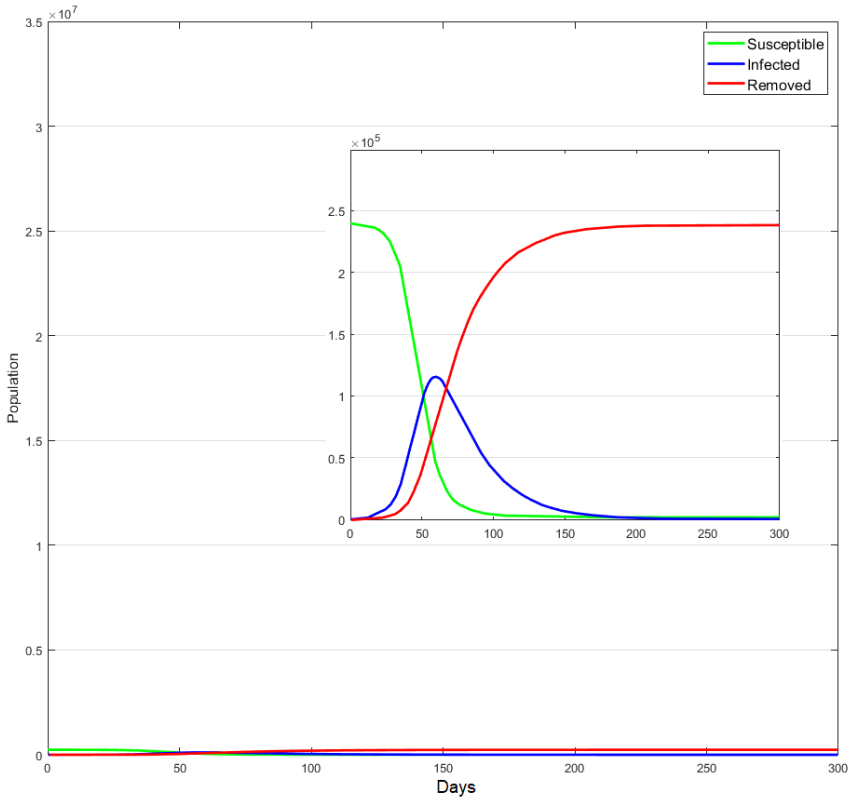

Figure 4.6. *The Cooper [49] model results recreated in Vensim.*

When attempting the Batistela [56] model on Vensim the results needed to be scaled by a factor, the population of each city, to achieve similar numbers to those in the paper. An explicit value for this factor was not given and could thus only be estimated. A total of 10 parameters were needed to recreate this model. Figure 4.7 shows the recreated results for the second and fourth fits for São Paulo.

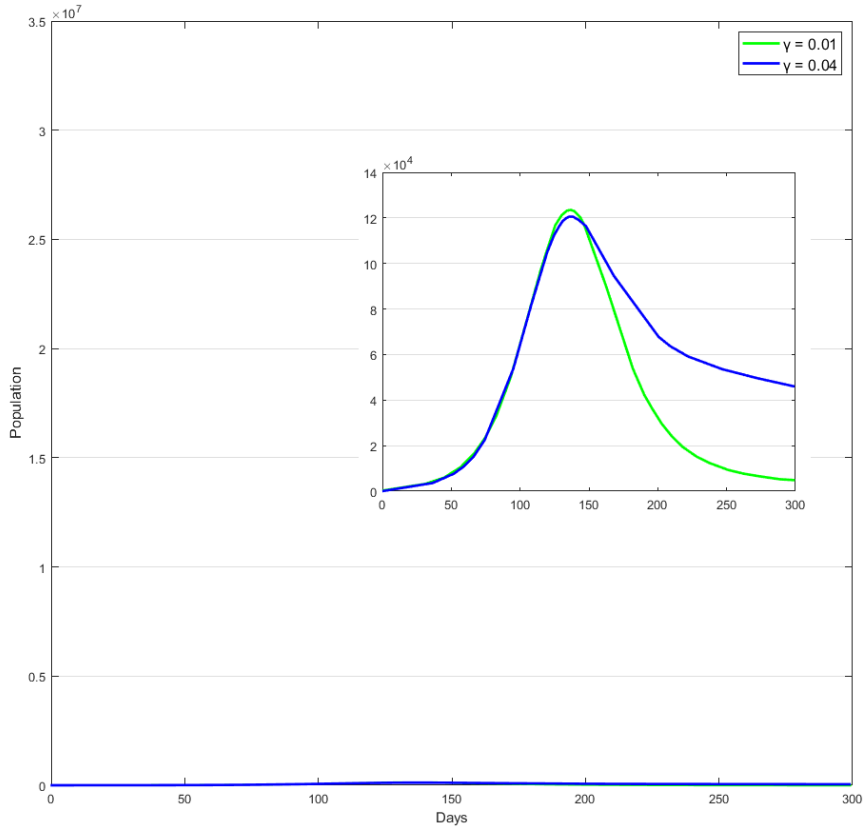

Figure 4.7. *The Batistela [56] model results for the Sick compartment recreated in Vensim with two sets of fitted parameters.*

5. DISCUSSION

Many models assumed an unchanging total population, which is a valid assumption considering the time windows used in the models were relatively short. Another assumption present with many of the models was making the whole population susceptible in the beginning, which would not be the case in most countries. The focus was largely on the early dynamics of the epidemic, meaning the models are not necessarily applicable in the present times. A high number of models took into account heterogeneity of the population in some way, such as by including multiple regions. The transmission rate was often time-varying, but the recovery or removal rates were typically constant. This is plausible, as control measures do affect the transmission rate of the virus, but the average duration of the illness would mostly stay the same and by extension, so would the recovery rate. Authors are aware that the classical SIR model is not an accurate modelling tool in the case of COVID-19, and many extended models were used. The asymptomatic carriers of the virus and fatalities were included in many models. Some models also considered the effectivity of control measures in another form than by altering the transmission rate, but thusfar no model had included the effect of vaccines. Surprisingly, only a minority of the models considered immunity loss which is a real possibility with the virus. Only one model took into account the possibility of a mutation of the virus, a phenomenon which has been reported in increasing numbers [66].

6. CONCLUSIONS

Mathematical models are a promising tool for forecasting the development of an epidemic and researchers are racing to create increasingly extensive models of COVID-19. With numerous studies on the subject being published each month, it is important to attain a view of the current scope of modelling. While the accuracy of the models presented has not been assessed, they could offer useful insight to the spread patterns of COVID-19 if maintained properly. Maintenance in this context would mean re-fitting the parameters periodically and including new aspects of the virus as needed. Many models presented did not include essential characteristics, such as the temporary immunity from infection and the mutated variants of the virus. COVID-19 models still need more development to truly portray the epidemic at hand. With vaccines against the virus coming out recently, there might not be a need for active modeling of the virus in the near future, but it is a good case study for the usability of the SIR model and its derivatives.

REFERENCES

[1] Organization, W. H. *Coronavirus disease (COVID-19) outbreak*. https://www.who.int/emergencies/diseases/novel-coronavirus-2019. Accessed: 2021-2-21.

[2] Ross, R. An application of the theory of probabilities to the study of a priori pathometry. —Part I. *Proc. R. Soc. A.* 92 (1916), pp. 204–230. URL: https://doi.org/10.1098/rspa.1916.0007.

[3] Hudson, H. P. and Ross, R. An Application of the theory of probabilities to the study of a priori pathometry. –Part II. *Proc. R. Soc. A.* 93 (1917), pp. 212–225. URL: https://doi.org/10.1098/rspa.1917.0014.

[4] Kermack, W. O. and McKendrick, A. G. A contribution to the mathematical theory of epidemics. *Proc. R. Soc. A.* 115 (1927), pp. 700–721. URL: https://doi.org/10.1098/rspa.1927.0118.

[5] Kermack, W. O. and McKendrick, A. G. Contributions to the mathematical theory of epidemics. II. – The problem of endemicity. *Proc. R. Soc. A.* 138 (1932), pp. 55–83. URL: https://doi.org/10.1098/rspa.1932.0171.

[6] Kermack, W. O. and McKendrick, A. G. Contributions to the mathematical theory of epidemics. III.–Further studies of the problem of endemicity. *Proc. R. Soc. A.* 141 (1933), pp. 86–94. URL: https://doi.org/10.1098/rspa.1933.0106.

[7] Ma, Z. and Li, J. *Dynamical Modeling And Analysis Of Epidemics*. Singapore: World Scientific Publishing Company, 2009. URL: https://doi.org/10.1142/6799.

[8] SeyedAlinaghi, S. et al. Reinfection risk of novel coronavirus (CoVID-19): A systematic review of current evidence. *World Journal of Virology* 9.5 (2020), pp. 79–90. URL: https://doi.org/10.5501/wjv.v9.i5.79.

[9] Katul, G. G. et al. Global convergence of COVID-19 basic reproduction number and estimation from early-time SIR dynamics. *PLOS ONE* 15.9 (2020), e0239800. URL: https://doi.org/10.1371/journal.pone.0239800.

[10] Sadurni, E. and Luna-Acosta, G. Exactly solvable SIR models, their extensions and their application to sensitive pandemic forecasting. *Nonlinear Dynamics* 103.3 (2021), pp. 2955–2971. URL: https://doi.org/10.1007/s11071-021-06248-y.

[11] Ahmetolan, S. et al. What Can We Estimate From Fatality and Infectious Case Data Using the Susceptible-Infected-Removed (SIR) Model? A Case Study of Covid-19 Pandemic. *Frontiers in Medicine* 7 (2020). URL: https://doi.org/10.3389/fmed.2020.556366.

[12] Al-Anzi, B. S. et al. An Overview of the World Current and Future Assessment of Novel COVID-19 Trajectory, Impact, and Potential Preventive Strategies at Healthcare Settings. *International Journal of Environmental Research and Public Health* 17.19 (2020), p. 7016. URL: https://doi.org/10.3390/ijerph17197016.

[13] Barlow, N. S. and Weinstein, S. J. Accurate closed-form solution of the SIR epidemic model. *Physica D: Nonlinear Phenomena* 408 (2020), p. 132540. URL: https://doi.org/10.1016/j.physd.2020.132540.

[14] Dos Santos, I. F. F. et al. Adaptive SIR model for propagation of SARS-CoV-2 in Brazil. *Physica A: Statistical Mechanics and its Applications* 569 (2021), p. 125773. URL: https://doi.org/10.1016/j.physa.2021.125773.

[15] Jung, S. Y. et al. Real-World Implications of a Rapidly Responsive COVID-19 Spread Model with Time-Dependent Parameters via Deep Learning: Model Development and Validation. *Journal of Medical Internet Research* 22.9 (2020), e19907. URL: https://doi.org/10.2196/19907.

[16] Lounis, M. and Bagal, D. K. Estimation of SIR model's parameters of COVID-19 in Algeria. *Bulletin of the National Research Centre* 44.1 (2020). URL: https://doi.org/10.1186/s42269-020-00434-5.

[17] Malavika, B. et al. Forecasting COVID-19 epidemic in India and high incidence states using SIR and logistic growth models. *Clinical Epidemiology and Global Health* 9 (2021), pp. 26–33. URL: https://doi.org/10.1016/j.cegh.2020.06.006.

[18] Miranda, J. G. V. et al. Scaling effect in COVID-19 spreading: The role of heterogeneity in a hybrid ODE-network model with restrictions on the inter-cities flow. *Physica D: Nonlinear Phenomena* 415 (2021), p. 132792. URL: https://doi.org/10.1016/j.physd.2020.132792.

[19] Nguemdjo, U. et al. Simulating the progression of the COVID-19 disease in Cameroon using SIR models. *PLOS ONE* 15.8 (2020), e0237832. URL: https://doi.org/10.1371/journal.pone.0237832.

[20] Srivastava, V. et al. A systematic approach for COVID-19 predictions and parameter estimation. *Personal and Ubiquitous Computing* (2020). URL: https://doi.org/10.1007/s00779-020-01462-8.

[21] Szapudi, I. Heterogeneity in SIR epidemics modeling: superspreaders and herd immunity. *Applied Network Science* 5.1 (2020). URL: https://doi.org/10.1007/s41109-020-00336-5.

[22] Turk, P. J. et al. Modeling COVID-19 Latent Prevalence to Assess a Public Health Intervention at a State and Regional Scale: Retrospective Cohort Study. *JMIR Public Health and Surveillance* 6 (2020), e19353. URL: https://doi.org/10.2196/19353.

[23] Abuhasel, K. A. et al. Analyzing and forecasting COVID-19 pandemic in the Kingdom of Saudi Arabia using ARIMA and SIR models. *Computational Intelligence* (2020). URL: https://doi.org/10.1111/coin.12407.

[24] Ambrosio, B. and Aziz-Alaoui, M. A. On a Coupled Time-Dependent SIR Models Fitting with New York and New-Jersey States COVID-19 Data. *Biology* 9.6 (2020), p. 135. URL: https://doi.org/10.3390/biology9060135.

[25] Amiri Mehra, A. H. et al. Parameter Estimation and Prediction of COVID-19 Epidemic Turning Point and Ending Time of a Case Study on SIR/SQAIR Epidemic Models. *Computational and Mathematical Methods in Medicine* 2020 (2020), pp. 1–13. URL: https://doi.org/10.1155/2020/1465923.

[26] Enrique Amaro, J. et al. Global analysis of the COVID-19 pandemic using simple epidemiological models. *Applied Mathematical Modelling* 90 (2021), pp. 995–1008. URL: https://doi.org/10.1016/j.apm.2020.10.019.

[27] Fanelli, D. and Piazza, F. Analysis and forecast of COVID-19 spreading in China, Italy and France. *Chaos, Solitons & Fractals* 134 (2020), p. 109761. URL: https://doi.org/10.1016/j.chaos.2020.109761.

[28] Fort, D. et al. Locally Informed Modeling to Predict Hospital and Intensive Care Unit Capacity During the COVID-19 Epidemic. *Ochsner Journal* 20.3 (2020), pp. 285–292. URL: https://doi.org/10.31486/toj.20.0073.

[29] Guirao, A. The Covid-19 outbreak in Spain. A simple dynamics model, some lessons, and a theoretical framework for control response. *Infectious Disease Modelling* 5 (2020), pp. 652–669. URL: https://doi.org/10.1016/j.idm.2020.08.010.

[30] Harb, A. M. and Harb, S. M. Corona COVID-19 spread - a nonlinear modeling and simulation. *Computers & Electrical Engineering* 88 (2020), p. 106884. URL: https://doi.org/10.1016/j.compeleceng.2020.106884.

[31] Ianni, A. and Rossi, N. Describing the COVID-19 outbreak during the lockdown: fitting modified SIR models to data. *The European Physical Journal Plus* 135.11 (2020). URL: https://doi.org/10.1140/epjp/s13360-020-00895-7.

[32] Law, K. B. et al. Tracking the early depleting transmission dynamics of COVID-19 with a time-varying SIR model. *Scientific Reports* 10.1 (2020). URL: https://doi.org/10.1038/s41598-020-78739-8.

[33] Mohamed, I. A. et al. A new model for epidemic prediction: COVID-19 in Kingdom Saudi Arabia case study. *Materials Today: Proceedings* (2021). URL: https://doi.org/10.1016/j.matpr.2021.01.088.

[34] Roda, W. C. et al. Why is it difficult to accurately predict the COVID-19 epidemic?: *Infectious Disease Modelling* 5 (2020), pp. 271–281. URL: https://doi.org/10.1016/j.idm.2020.03.001.

[35] Rubin, D. M. et al. Facilitating Understanding, Modeling and Simulation of Infectious Disease Epidemics in the Age of COVID-19. *Frontiers in Public Health* 9 (2021), p. 33. URL: https://doi.org/10.3389/fpubh.2021.593417.

[36] Wangping, J. et al. Extended SIR Prediction of the Epidemics Trend of COVID-19 in Italy and Compared With Hunan, China. *Frontiers in Medicine* 7 (2020). URL: https://doi.org/10.3389/fmed.2020.00169.

[37] Zareie, B. et al. A Model for COVID-19 Prediction in Iran Based on China Parameters. *Archives of Iranian Medicine* 23.4 (2020), pp. 244–248. URL: https://doi.org/10.34172/aim.2020.05.

[38] Alanazi, S. A. et al. Measuring and Preventing COVID-19 Using the SIR Model and Machine Learning in Smart Health Care. *Journal of Healthcare Engineering* 2020 (2020), pp. 1–12. URL: https://doi.org/10.1155/2020/8857346.

[39] Calafiore, G. C. et al. A time-varying SIRD model for the COVID-19 contagion in Italy. *Annual Reviews in Control* 50 (2020), pp. 361–372. URL: https://doi.org/10.1016/j.arcontrol.2020.10.005.

[40] Predicting intervention effect for COVID-19 in Japan: state space modeling approach. *Bioscience Trends* 14 (2020), pp. 174–181. URL: https://doi.org/10.5582/bst.2020.03133.

[41] Kolokolnikov, T. and Iron, D. Law of mass action and saturation in SIR model with application to Coronavirus modelling. *Infectious Disease Modelling* 6 (2021), pp. 91–97. URL: https://doi.org/10.1016/j.idm.2020.11.002.

[42] Maier, B. F. and Brockmann, D. Effective containment explains subexponential growth in recent confirmed COVID-19 cases in China. *Science* 368.6492 (2020), pp. 742–746. URL: https://doi.org/10.1126/science.abb4557.

[43] Moussaoui, A. and Zerga, E. H. Transmission dynamics of COVID-19 in Algeria: The impact of physical distancing and face masks. *AIMS Public Health* 7.4 (2020), pp. 816–827. URL: https://doi.org/10.3934/publichealth.2020063.

[44] Peng, T. et al. City lockdown and nationwide intensive community screening are effective in controlling the COVID-19 epidemic: Analysis based on a modified SIR model. *PLOS ONE* 15.8 (2020), e0238411. URL: https://doi.org/10.1371/journal.pone.0238411.

[45] Prodanov, D. Parameter Estimation of the SIR Epidemic Model. Applications to the COVID-19 Pandemic. *Entropy* 23 (2020), p. 59. URL: https://doi.org/10.3390/e23010059.

[46] Rocchi, E. et al. A Possible Scenario for the Covid-19 Epidemic, Based on the SI(R) Model. *SN Comprehensive Clinical Medicine* 2.5 (2020), pp. 501–503. URL: https://doi.org/10.1007/s42399-020-00306-z.

[47] Piecewise quadratic growth during the 2019 novel coronavirus epidemic. *Infectious Disease Modelling* 5 (2020), pp. 681–690. URL: https://doi.org/10.1016/j.idm.2020.08.014.

[48] Brugnano, L. et al. A multiregional extension of the SIR model, with application to the COVID-19 spread in Italy. *Mathematical Methods in the Applied Sciences* 44.6 (2020), pp. 4414–4427. URL: https://doi.org/10.1002/mma.7039.

[49] Cooper, I. et al. Dynamic tracking with model-based forecasting for the spread of the COVID-19 pandemic. *Chaos, Solitons & Fractals* 139 (2020), p. 110298. URL: https://doi.org/10.1016/j.chaos.2020.110298.

[50] Modeling the epidemic dynamics and control of COVID-19 outbreak in China. *Quantitative Biology* 8 (2020), pp. 11–19. URL: https://doi.org/10.1007/s40484-020-0199-0.

[51] Bastos, S. B. and Cajueiro, D. O. Modeling and forecasting the early evolution of the Covid-19 pandemic in Brazil. *Scientific Reports* 10.1 (2020). URL: https://doi.org/10.1038/s41598-020-76257-1.

[52] Berestycki, H. et al. Propagation of Epidemics Along Lines with Fast Diffusion. *Bulletin of Mathematical Biology* 83.1 (2020). URL: https://doi.org/10.1007/s11538-020-00826-8.

[53] Nakamura, G. et al. Effective epidemic model for COVID-19 using accumulated deaths. *Chaos, Solitons & Fractals* 144 (2021), p. 110667. URL: https://doi.org/10.1016/j.chaos.2021.110667.

[54] Karaivanov, A. A social network model of COVID-19. *PLOS ONE* 15.10 (2020), e0240878. URL: https://doi.org/10.1371/journal.pone.0240878.

[55] Neves, A. G. M. and Guerrero, G. Predicting the evolution of the COVID-19 epidemic with the A-SIR model: Lombardy, Italy and São Paulo state, Brazil. *Physica D: Nonlinear Phenomena* 413 (2020), p. 132693. URL: https://doi.org/10.1016/j.physd.2020.132693.

[56] Batistela, C. M. et al. SIRSi compartmental model for COVID-19 pandemic with immunity loss. *Chaos, Solitons & Fractals* 142 (2021), p. 110388. URL: https://doi.org/10.1016/j.chaos.2020.110388.

[57] Tomochi, M. and Kono, M. A mathematical model for COVID-19 pandemic—SIIR model: Effects of asymptomatic individuals. *Journal of General and Family Medicine* 22.1 (2020), pp. 5–14. URL: https://doi.org/10.1002/jgf2.382.

[58] Venkatasen, M. et al. Forecasting of the SARS-CoV-2 epidemic in India using SIR model, flatten curve and herd immunity. *Journal of Ambient Intelligence and Humanized Computing* (2020). URL: https://doi.org/10.1007/s12652-020-02641-4.

[59] Muñoz-Fernández, G. A. et al. A SIR-type model describing the successive waves of COVID-19. *Chaos, Solitons & Fractals* 144 (2021), p. 110682. URL: https://doi.org/10.1016/j.chaos.2021.110682.

[60] Carli, R. et al. Model predictive control to mitigate the COVID-19 outbreak in a multi-region scenario. *Annual Reviews in Control* 50 (2020), pp. 373–393. URL: https://doi.org/10.1016/j.arcontrol.2020.09.005.

[61] Peng, Z. et al. Estimating Unreported COVID-19 Cases with a Time-Varying SIR Regression Model. *International Journal of Environmental Research and Public Health* 18.3 (2021), p. 1090. URL: https://doi.org/10.3390/ijerph18031090.

[62] Colombo, R. M. et al. An age and space structured SIR model describing the Covid-19 pandemic. *Journal of Mathematics in Industry* 10.1 (2020). URL: https://doi.org/10.1186/s13362-020-00090-4.

[63] Ibarra-Vega, D. Lockdown, one, two, none, or smart. Modeling containing covid-19 infection. A conceptual model. *Science of The Total Environment* 730 (2020), p. 138917. URL: https://doi.org/10.1016/j.scitotenv.2020.138917.

[64] Ferchiou, A. et al. Individual Behaviors and COVID-19 Lockdown Exit Strategy: A Mid-Term Multidimensional Bio-economic Modeling Approach. *Frontiers in Public Health* 8 (2020). URL: https://doi.org/10.3389/fpubh.2020.606371.

[65] Ramos, A. M. et al. A simple but complex enough theta-SIR type model to be used with COVID-19 real data. Application to the case of Italy. *Physica D: Nonlinear Phenomena* (2021), p. 132839. URL: https://doi.org/10.1016/j.physd.2020.132839.

[66] Plante, J. A. et al. The variant gambit: COVID-19's next move. *Cell Host & Microbe* 29.4 (2021), pp. 508–515. URL: https://doi.org/10.1016/j.chom.2021.02.020.

[67] Alqahtani, R. T. Mathematical model of SIR epidemic system (COVID-19) with fractional derivative: stability and numerical analysis. *Advances in Difference Equations* 2021.1 (2021). URL: https://doi.org/10.1186/s13662-020-03192-w.

[68] Al-Khani, A. M. et al. The SARS-CoV-2 pandemic course in Saudi Arabia: A dynamic epidemiological model. *Infectious Disease Modelling* 5 (2020), pp. 766–771. URL: https://doi.org/10.1016/j.idm.2020.09.006.

[69] Ben Hassen, H. et al. A SIR-Poisson Model for COVID-19: Evolution and Transmission Inference in the Maghreb Central Regions. *Arabian Journal for Science and Engineering* 46 (2020), pp. 93–102. URL: https://doi.org/10.1007/s13369-020-04792-0.

[70] Croccolo, F. and Roman, H. E. Spreading of infections on random graphs: A percolation-type model for COVID-19. *Chaos, Solitons & Fractals* 139 (2020), p. 110077. URL: https://doi.org/10.1016/j.chaos.2020.110077.

[71] De Oliveira, A. C. S. et al. Bayesian modeling of COVID-19 cases with a correction to account for under-reported cases. *Infectious Disease Modelling* 5 (2020), pp. 699–713. URL: https://doi.org/10.1016/j.idm.2020.09.005.

[72] Hussain, S. et al. Stochastic mathematical model for the spread and control of Corona virus. *Advances in Difference Equations* 2020 (2020). URL: https://doi.org/10.1186/s13662-020-03029-6.

[73] Janiak, A. et al. Covid-19 contagion, economic activity and business reopening protocols. *Journal of Economic Behavior & Organization* 182 (2021), pp. 264–284. URL: https://doi.org/10.1016/j.jebo.2020.12.016.

[74] Analysis of COVID-19 infection spread in Japan based on stochastic transition model. *Bioscience Trends* 14 (2020), pp. 134–138. URL: https://doi.org/10.5582/bst.2020.01482.

[75] Kudryashov, N. A. et al. Analytical features of the SIR model and their applications to COVID-19. *Applied Mathematical Modelling* 90 (2021), pp. 466–473. URL: https://doi.org/10.1016/j.apm.2020.08.057.

[76] Kurita, J. et al. Estimated effectiveness of school closure and voluntary event cancellation as COVID-19 countermeasures in Japan. *Journal of Infection and Chemotherapy* 27.1 (2021), pp. 62–64. URL: https://doi.org/10.1016/j.jiac.2020.08.012.

[77] Liao, Z. et al. TW-SIR: time-window based SIR for COVID-19 forecasts. *Scientific Reports* 10.1 (2020). URL: https://doi.org/10.1038/s41598-020-80007-8.

[78] Liu, X. A simple, SIR-like but individual-based epidemic model: Application in comparison of COVID-19 in New York City and Wuhan. *Results in Physics* 20 (2021), p. 103712. URL: https://doi.org/10.1016/j.rinp.2020.103712.

[79] Lymperopoulos, I. N. #stayhome to contain Covid-19: Neuro-SIR – Neurodynamical epidemic modeling of infection patterns in social networks. *Expert Systems with Applications* 165 (2021), p. 113970. URL: https://doi.org/10.1016/j.eswa.2020.113970.

[80] Maheshwari, P. and Albert, R. Network model and analysis of the spread of Covid-19 with social distancing. *Applied Network Science* 5.1 (2020). URL: https://doi.org/10.1007/s41109-020-00344-5.

[81] Pizzuti, C. et al. Network-based prediction of COVID-19 epidemic spreading in Italy. *Applied Network Science* 5.1 (2020). URL: https://doi.org/10.1007/s41109-020-00333-8.

[82] Postnikov, E. B. Estimation of COVID-19 dynamics "on a back-of-envelope": Does the simplest SIR model provide quantitative parameters and predictions?: *Chaos, Solitons & Fractals* 135 (2020), p. 109841. URL: https://doi.org/10.1016/j.chaos.2020.109841.

[83] Prasse, B. et al. Network-inference-based prediction of the COVID-19 epidemic outbreak in the Chinese province Hubei. *Applied Network Science* 5.1 (2020). URL: https://doi.org/10.1007/s41109-020-00274-2.

[84] Ray, D. et al. Predictions, Role of Interventions and Effects of a Historic National Lockdown in India's Response to the the COVID-19 Pandemic: Data Science Call to Arms. *Harvard Data Science Review* (2020). URL: https://doi.org/10.1162/99608f92.60e08ed5.

[85] Sharov, K. S. Creating and applying SIR modified compartmental model for calculation of COVID-19 lockdown efficiency. *Chaos, Solitons & Fractals* 141 (2020), p. 110295. URL: https://doi.org/10.1016/j.chaos.2020.110295.

[86] Taghvaei, A. et al. Fractional SIR epidemiological models. *Scientific Reports* 10.1 (2020). URL: https://doi.org/10.1038/s41598-020-77849-7.

[87] Vattay, G. Forecasting the outcome and estimating the epidemic model parameters from the fatality time series in COVID-19 outbreaks. *Physical Biology* 17.6 (2020), p. 065002. URL: https://doi.org/10.1088/1478-3975/abac69.

[88] Vyklyuk, Y. et al. Modeling and analysis of different scenarios for the spread of COVID-19 by using the modified multi-agent systems – Evidence from the selected countries. *Results in Physics* 20 (2021), p. 103662. URL: https://doi.org/10.1016/j.rinp.2020.103662.

[89] Wacker, B. and Schluter, J. Time-continuous and time-discrete SIR models revisited: theory and applications. *Advances in Difference Equations* (2020). URL: https://doi.org/10.1186/s13662-020-02995-1.

[90] Zhou, T. and Ji, Y. Semiparametric Bayesian inference for the transmission dynamics of COVID-19 with a state-space model. *Contemporary Clinical Trials* 97 (2020), p. 106146. URL: https://doi.org/10.1016/j.cct.2020.106146.

[91] Zreiq, R. et al. Generalized Richards model for predicting COVID-19 dynamics in Saudi Arabia based on particle swarm optimization Algorithm. *AIMS Public Health* 7.4 (2020), pp. 828–843. URL: https://doi.org/10.3934/publichealth.2020064.

APPENDIX A: TABLE OF RESULTS

Table A.1. *The collection of papers reviewed in an order of increasing number of parameters.*

Authors	**Model**	**Parameters**	**Values**	**Notes**
Katul et al. [9]	SIR	Basic reproduction number R_0	$R_0 = 4.5$	A normalized SIR model.
Sadurní and Luna-Acosta [10]	SIR	Control parameter κ	-	The model is reduced to a one-variable system.
Ahmetolan et al. [11]	SIR	Basic reproduction number R_0 Mean infectious period T	$1.5 < R_0 < 10$ $2 < T < 30$	-
Al-anzi et al. [12]	SIR	Infection rate β Recovery rate γ	-	They used a MATLAB SIR modeling tool.
Barlow and Weinstein [13]	SIR	Transmission rate r recovery rate α	$r = 2.9236 \times 10^{-5}$ $\alpha = 0.0164$	A closed-form solution of the model.
Dos Santos et al. [14]	SIR	Transmission rate β Recovery rate γ	$\beta \in [0.05, 0.6]$ $\gamma \in [0.07, 0.13]$	Includes time-varying parameters.

Jung et al. [15]	SIR	Infection rate β Recovery rate γ	$\beta = 0.1656$ $\gamma = 0.0253$	Features time-varying parameters and a neural network model.
Lounis and Bagal [16]	SIR	Transmission rate β Removal rate γ	$\beta = 0.0561215$ $\gamma = 0.0455331$	Adds nothing new.
Malavika et al. [17]	SIR	Transmission parameter β Recovery rate γ	$\beta = 0.36$ $\gamma = 0.14$	A short-term model.
Miranda et al. [18]	Hybrid SIR	Transmission rates $\beta_{i,s,c}$ Recovery rate γ_i	-	Combines SIR equations and a network diffusion model.
Nguemdjo et al. [19]	SIR	Effective contact rate β Removal rate γ	$\beta = 0.615$ $\gamma = 0.393$	Adds nothing new.
Srivastava et al. [20]	SIR	Contact rate r Recovery rate a	$r = 0.0096$ $a = 0.1006$	Considers the effects of lockdown.
Szapudi [21]	SIR	Infection probability β Recovery rate γ	$\beta = 0.07$ $\gamma = 0.1$	Includes heterogeneity.
Turk et al. [22]	SIR	Infection rate β Removal rate γ	$\beta = 0.6415, 0.6165, 0.7020, 0.6381$ $\gamma = 0.3585, 0.3835, 0.2980, 0.3619$	Fitted parameters twice for each region.
Abuhasel et al. [23]	SIR	Contact rate β Recovery rate γ	$\beta = 0.133$ $\gamma = \frac{1}{14}$	Adds nothing new.

		Total population N	$N = 34,806,116$	
Ambrosio and Aziz-Alaoui [24]	SIRD	Infection rate $k(t)$ Recovery rate r Death rate $d(t)$	$k \in [0.67, 1.057]$ $r = 0.64$ $d \in [0.0016, 0.00232]$	The infection and death rates are adjusted over time.
Amiri Mehra et al. [25]	SIRD	Transmission rate β Recovery rate g Removal rate μ_d	$\beta = 1$ $g = 0.223$ $\mu_d = 0.0261$	Adds nothing new.
Enrique Amaro et al. [26]	SID	Theoretical number of deaths a Characteristic evolution time b Inverse dead factor c	-	Does not consider recoveries.
Fanelli and Piazza [27]	SIRD	Infection rate r Recovery rate a Death rate d	$r = 7.9 \times 10^{-6}, 3.33 \times 10^{-6}$ $a = 2.13 \times 10^{-2}, 1.8 \times 10^{-2}$ $d = 1.63 \times 10^{-2}, 3 \times 10^{-3}$	Adds nothing new.
Fort et al. [28]	SIR	Basic reproduction number R_0 Contacts β Inverse recovery time γ	-	Considers many additional groups.

Guirao [29]	SEIR	Reproductive number r_0 Infection period τ_i Latent period τ_l	$\tau_i = 1.63, 2.56$ $\tau_l = 3.0, 2.0$	-
Harb and Harb [30]	SIRD	Contact factor b Transmit factor a Health medication quality factor m	-	Considers the medication quality factor.
Ianni and Rossi [31]	SIRD	Transmission rate $\beta(t)$ Recovery rate γ_R Mortality rate γ_D	$\beta_0 = \frac{1}{1.8}, \frac{1}{2.2}$ $\gamma_R = \frac{1}{41}$ $\gamma_D = \frac{1}{145}$	Time variant parameters included.
Law et al. [32]	SIR	Fraction parameter z Proportion of depletion p Removal rate δ	$z = 0.4374$ $0.3914, 0.4047$ $p = 0.0784,$ $0.0450, 0.0466$ $\delta = 0.025,$ $0.042, 0.050$	Features a time variant infection rate.
Mohamed et al. [33]	MSIR	Infection rate β Recovery rate γ Number of unaffected people α	-	Immunity-Susceptible-Infected-Recovered model.
Roda et al. [34]	SIR	Transmission rate β	$\beta = 9.906 \times 10^{-8}$	R denotes the confirmed cases.

		Diagnosis rate ρ Recovery rate μ	$\rho = 0.24$ $\mu = 0.1$	
Rubin et al. [35]	SIIR	Transmission constant β Recovery constant γ Infectiousness multiplier	$\beta = 0.19$ $\gamma = 0.125$ 1.5	Considers a mutation of the virus.
Wangping et al. [36]	SIR	Transmission rate β Removal rate γ Transmission modifier $\pi(t)$	-	Includes time-varying transmission rates.
Zareie et al. [37]	SIRD	Transmission rate $\beta(t)$ Recovery rate $Y(t)$ Death rate $\mu(t)$	-	Includes time-dependent parameters.
Alanazi et al. [38]	SIRD	Effective contact rate β Mortality rates $\alpha_{1,2}$ Recovery rate γ	$\beta = 0.1$ $\alpha_1 = 0.018$ $\alpha_2 = \frac{1}{47464}$ $\gamma = \frac{1}{17}$	-
Calafiore et al. [39]	SIRD	Infection rate $\beta(t)$ Recovery rate $\gamma(t)$ Death rate $\nu(t)$ Scalar parameter $q(t)$	$\beta \in [0.63, 0]$ $\gamma \in [0, 0.048]$ $\nu \in [0, 0.08]$ $q \in [0, 1]$	Includes time-varying parameters.

Ianni and Rossi [31]	SIIR	Transmission rates $\beta_{S,A}(t)$ Recovery rates $\gamma_{S,A}$	$\beta_A = \frac{1}{7}$ $\gamma_S = \frac{1}{41}$ $\gamma_A = \frac{1}{78}$	Includes time variant parameters and considers asymptomatic cases.
Kobayashi et al. [40]	SIR	Infection rate β Removal rate γ Randomness parameters κ, λ	-	SIR combined with a space-state model.
Kolokolnikov and Iron [41]	SIR	Infection parameter α Recovery rate γ Rate of interaction μ Total population N	$\alpha = 15050$ $\gamma = 0.0232$ $\mu = 1.25 \times 10^{-5}$ $N = 7.7 \times 10^9$	Considers a spatial distribution of population.
Maier and Brockmann [42]	SIRQ	Basic reproduction number R_0 Infection period T_I Containment rates k, k_0	$R_0 = 6.2$ $T_I = 8$	A Susceptible-Infected-Recovered-Quarantined model.
Moussaoui and Zerga [43]	SIR	Basic reproduction number R_0 Proportion wearing masks m Degree of protection e	-	Considers invervention strategies.

		Proportion distancing d		
Peng et al. [44]	SIR	Effective contacts λ Infection probability p Recovery rate μ Proportion of unquarantined α	$\lambda = 5$ $p = 0.040$ $\mu = \frac{1}{14}$	Considers the proportion of unquarantined individuals.
Prodanov [45]	SIR	Inverse of reproductive number $g = \frac{\gamma}{\beta}$ Reproductive number R_0 Apparent peak i_m Apparent peak time T	-	Uses normalized variables and considers two waves.
Rocchi et al. [46]	SIR	Infection rate α Removal rate β Immunity loss rate ρ Proportion of symptomatic p	$\alpha = 0.6$ $\beta = 0.1$ $\rho \in [0.003, 0.006]$ $p \in [0.01, 0.10]$	Considers immunity loss and presymptomatic individuals.
Roda et al. [34]	SEIR	Transmission rate β Diagnosis rate ρ Recovery rate μ Transfer rate from E to I ϵ	$\beta = 8.68 \times 10^{-8}$ $\rho = 0.018$ $\mu = 0.1$ $\epsilon = 0.631$	A Susceptible-Exposed-Infected-Confirmed model.

Amiri Mehra et al. [25]	SIIRQ	Transmission rate β Transfer rate α Recovery rate g Removal rate μ_d Quarantine rate ϕ	$\beta = 1$ $\alpha = 0.214$ $g = 0.222$ $\mu_d = 0.0257$ $\phi = 0.95$	Considers presymptomatic and quarantined individuals.
Brandenburg [47]	SIR	Reproduction rate λ Recovery rate μ Diffusion constant κ Spatial and temporal coordinates x, t	-	A model with a spatial extension.
Brugnano et al. [48]	SIIR	Infection rate β_i Removal rates $\gamma_{i1,i2}$ Detection probability σ_i Delay time τ	$\gamma_1 = 0.043$ $\tau = 10$	Includes diagnosed and undiagnosed cases, and multiregionality.
Cooper et al. [49]	SIRD	Transmission rate a Removal rate b Death constants D_0, k_0 Scaling coefficient f	$a = 0.18$ $b = 0.037$ $D_0 = 3.6 \times 10^4$ $k_0 = 1.6 \times 10^{-5}$	The susceptible population could be increased in surges.

			$f = 2.4 \times 10^5$	
Zhao and Chen [50]	SUQC	Infection rate α Quarantine rate γ_1 Confirmation rates γ_2, σ, δ	$\alpha = 0.2967$ $\gamma_1 = 0.3357$ 0.0906	A Susceptible-Unquarantined-Quarantined-Confirmed model.
Bastos and Cajueiro [51]	SIIRD	Proportion of symptomatic p Infection rates $\beta_{A,S}$ Removal rates $\gamma_{A,S}$ Death probability ρ Effectiveness of social distancing ψ	$p = 0.3210$ $\beta_{A,S} = 0.4417$ $\gamma_A = 0.1260$ $\gamma_S = 0.1508$ $\rho = 0.0347$ $\psi \in [0, 1]$	A portion of the infected are asymptomatic.
Berestycki et al. [52]	SIRT	Diffusion coefficients d, D Transmission rate β Recovery rate α Exchange coefficients μ, ν	-	Population diffusion is included.
Nakamura et al. [53]	SIRD	Transmission rate β Removal rate λ Mortality rate f Sigmoid parameters τ, g_∞, b	-	The model is reduced to a single first-order differential equation.

Karaivanov [54]	SEIRD	Infectivity rate β	$\beta = 0.5$	A network-augmented SEIRD model.
		Removal rate r	$r = 0.2$	
		Mortality rate μ	$\mu = 0.0037r$	
		Recovery rate γ	$\gamma = r - \mu$	
		Incubation σ	$\sigma = \frac{1}{5.2}$	
		Mass testing rate θ	$\theta = 2\%, 5\%$	
		Contact tracing rate ϕ	$\phi = 10\%$	
Neves and Guerrero [55]	SIIRD	Infection rate β_0	-	Considers the asymptomatic
		Reduction factor μ		population and control measures.
		Probability of symptoms ξ		
		Removal rates $\gamma_{s,a}$		
		Case fatality rate ω		
		Measure intensity ϵ		
Batistela et al [56]	SIIR	Birth rate λ	$\lambda = 3.595 \times 10^{-5}$	Considers immunity loss,
		Death rate δ	$\delta = 1.822 \times 10^{-5}$	asymptomatics and the effect
		Infection rate α	$\alpha = 0.9377$	of social distancing.
		Removal rate σ	$\sigma = 0.1117$	
		Recovery rates $\beta_{1,3}$	$\beta_1 = 0.1181$	

		Diagnosis rate β_2 Effect of social distancing θ Immunity loss rate γ	$\beta_2 = 0.2978$ $\beta_3 = 0.06325$ $\theta = 0.5005$ $\gamma = 3.595 \times 10^{-5}$	
Tomochi and Kono [57]	SIIR	Infection probability $beta$ Transfer rates $b_1, b_2,$ c_1, c_2, c_3 Inverse of antibody duration d_1 Incubation period t_1 Onset period t_2	$\beta = 0.16$ $b_1 = 0.012$ $b_2 = 0.188$ $c_1 = \frac{1}{17}$ $c_2 = \frac{0.942}{17}$ $c_3 = \frac{1}{17} - \frac{0.942}{17}$ $d_1 = 0$ $t_1 = 5$ $t_2 = 17$	Considers presymptomatic individuals and couples two SIIR systems.
Venkatasen et al. [58]	SIRD	Fraction susceptible Contact success rate Infected contacts Contact rate Duration Transmission rate Growth rate Reproduction ratio Fatality rate	- 0.1 - 10 14 - 0.28	-
Muñoz-Fernández	SIR	Transmission rate β	-	Includes non-constant transfer

et al. [59]		Death rate μ' Recuperation rate γ Birth rate λ Death rate μ Coefficients $a_{\beta,\mu'}, b_{\beta,\mu'}$		rates and a general birth and death rate.
Carli et al. [60]	SIRQTHE	Infection rate $\beta(k)_i$ Diagnosis rate θ_i Healing rates $\gamma_i, \delta_i, \pi_i$ Hospitalization rate λ_i, μ_i Death rate ϵ_i Migration coefficient $\xi_{i,j}$ Control actions u_i, r_i	$U_i = [0, 0.2, 0.8]$ $R_i = [0, 1]$	A multi-regional Susceptible-Infected-Removed-Quarantined-Threatened-Healed-Extinct model.
Peng et al. [61]	SIIR	Infection rate β Recovery/death rate λ Unreported infection rates ϕ, ϕ' Coefficients a, b, c, d Constants m, n, k	-	Includes a time variant undocumented infection rate.
Colombo et al. [62]	SIHR	Hospitalization/ quarantining	-	susceptible-Infected-

		rate κ Recovery rates θ, η Mortality rates $\mu S, I, H, R$ Disease transmission ρ Position variables x, ξ Age variables a, α		Hospitalized-Recovered model with age and space dependent parameters
Ibarra-Vega [63]	SIRD	Contacts rate μ Fatality rate Fr Hospital capacity strain index HiC Incubation time it Disease duration Dd Fraction requiring hospitalization Fh Infectivity β Hospital capacity HC Lockdown effectivity λ Smart lockdown effectivity k Post lockdown effectivity q Serious cases SC	-	Takes into account hospitalization and lockdowns.

Ferchiou et al. [64]	SEIH-ICU-RD	Incubation period θ^{-1}	$\theta^{-1} = 5.2$	Susceptible-Exposed
		Prodromal phase duration μ_p^{-1}	$\mu_p^{-1} = 1.5$	-Infected-Hospitalized-
		Latency period ϵ^{-1}	$\epsilon^{-1} = \theta^{-1} - \mu_p^{-1}$	Intensive care-
		Probability of being	$Pa = 0.2$	Recovered-Dead model.
		asymptomatic Pa	$Pps = 1, 0.2$	
		Probability of being	$Pms = 0, 0.7, 0.6$	
		paucisymptomatic Pps	$Pss = 0, 0.1, 0.2$	
		Probability of mild	$s = 7.5$	
		symptoms Pms	μ^{-1} = 2.3	
		Probability of severe	$r_\beta = 0.51$	
		symptoms Pss	$pICU = 0, 0.36, 0.2$	
		Serial interval s	$\lambda_{H,R} = 0, 0.072,$	
		Infectious period μ^{-1}	0.022	
		Relative infectiousness r_β	$\lambda_{ICU,R} = 0, 0.05,$	
		Probability of going	0.036	
		in ICU $pICU$	$\lambda_{H,D} = 0, 0.0042,$	
		Daily recovery rates $\lambda_{H,R}, \lambda_{ICU,R}$	0.014	
		Daily death rates $\lambda_{H,D}, \lambda_{ICU,D}$	$\lambda_{ICU,D} = 0, 0.0074,$ 0.029	

Ramos et al. [65]	θ-SEIHQRD	Population N	$N = 60,317,000$	Susceptible-Exposed-Infected-
		Transition rates $\gamma_E, \gamma_I(t), \gamma_{I_u}(t),$	$\gamma_E = \frac{1}{5.5}$	Hospitalized-Quarantined-
		$\gamma_{H_R}(t), \gamma_{H_D}(t),$	$\gamma_I(t) = \frac{1}{5}$	Recovered-Dead model.
		$\gamma_{I_{Du}}(t), \gamma_{Q,1}, \gamma_{Q,2}$	$\gamma_{I_u}(t) = \frac{1}{9}$	
		Disease contact rates $\beta_{I,0}, \beta_{I_{Du},0}$	$\gamma_{H_R}(t) = \frac{1}{14.2729}$	
		β_{H_R}, β_{H_D}	$\gamma_{H_D}(t) = \frac{1}{5}$	
		Instantaneous infection undetected	$\gamma_{I_{Du}}(t) = \infty$	
		fatality ratios $\omega_{u,0}, \omega_{u,1}, \omega_{u,2}$	$\gamma_{Q,1} = \frac{1}{36.0450}$	
		Proportion of undetected	$\gamma_{Q,2} = \frac{1}{24.8646}$	
		infections $\theta(t)$	$\beta_{I,0} = 0.4992$	
		Ratio of new detected	$\omega_{u,0}, \omega_{u,1} = 0.42$	
		infected who will recover	$\omega_{u,2} = 0$	
		after hospitalization p_0	$p_0 = 0.7382$	
Excluded				
Alqahtani [67]	-	-	-	Includes a non-linear incidence rate.
Al-Khani et al. [68]	-	-	-	Unclear model characteristics.
Ben Hassen et al. [69]	-	-	-	A Poisson model.

Croccolo et al. [70]	-	-	-	Focused on a network model.
De Oliveira et al. [71]	-	-	-	A Bayesian model.
Hussain et al. [72]	-	-	-	Stochastic model, not comparable.
Janiak et al. [73]	-	-	-	Focuses on business reopening protocols.
Karako et al. [74]	-	-	-	A stochastic model, not SIR.
Kudryashov et al. [75]	-	-	-	Mathematical analysis that is not applicable to our purposes.
Kurita et al. [76]	-	-	-	Model was not presented.
Liao et al. [77]	-	-	-	Not applicable.
Liu [78]	-	-	-	Not actually a SIR model.
Lympero- poulos [79]	-	-	-	A neurodynamical SIR that is not comparable.
Maheshwari and Albert [80]	-	-	-	Presents a network SIR not applicable for our purposes.

Pizzuti et al. [81]	-	-	-	Not a SIR model.
Postnikov [82]	-	-	-	Uses Verhulst logistic equations.
Prasse et al. [83]	-	-	-	Not comparable.
Ray et al. [84]	-	-	-	A Bayesian extension.
Sharov [85]	-	-	-	Differs too much from SIR models.
Taghvaei et al. [86]	-	-	-	A fractional model.
Vattay [87]	-	-	-	An explicit single variable differential equation for deaths.
Vyklyuk et al. [88]	-	-	-	Not comparable as a SIR model.
Wacker and Schlüter [89]	-	-	-	Not comparable.
Zhou and Ji [90]	-	-	-	Bayesian model.
Zreiq et al. [91]	-	-	-	Does not focus on the SIR model.